Large amplitude spin torque vortex oscillations at zero external field using a perpendicular spin polarizer

A. Dussaux, E. Grimaldi, B. Rache Salles, A. S. Jenkins, A. V. Khvalkovskiy, P. Bortolotti, J. Grollier, H. Kubota, A. Fukushima, K. Yakushiji, S. Yuasa, V. Cros, and A. Fert

Citation: Applied Physics Letters **105**, 022404 (2014); doi: 10.1063/1.4885537
View online: http://dx.doi.org/10.1063/1.4885537
View Table of Contents: http://scitation.aip.org/content/aip/journal/apl/105/2?ver=pdfcov
Published by the AIP Publishing

Large amplitude spin torque vortex oscillations at zero external field using a perpendicular spin polarizer

A. Dussaux,[1,a)] E. Grimaldi,[1,2,b)] B. Rache Salles,[1,c)] A. S. Jenkins,[1,d)] A. V. Khvalkovskiy,[1,3,e)] P. Bortolotti,[1] J. Grollier,[1] H. Kubota,[4] A. Fukushima,[4] K. Yakushiji,[4] S. Yuasa,[4] V. Cros,[1] and A. Fert[1]

[1]*Unité Mixte de Physique CNRS/Thales and Université Paris Sud 11, 1 Ave. A. Fresnel, 91767 Palaiseau, France*

[2]*CNES, 1 Avenue Edouard Belin, 31400 Toulouse, France*

[3]*A.M. Prokhorov General Physics Institute of RAS, Vavilova Str. 38, 119991 Moscow, Russia*

[4]*National Institute of Advanced Industrial Science and Technology (AIST), Tsukuba, Japan*

(Received 8 April 2014; accepted 16 June 2014; published online 14 July 2014)

We investigate the microwave response of a spin transfer vortex based oscillator in a magnetic tunnel junction with an in-plane reference layer combined with a spin valve with an out-of-plane magnetization spin polarizing layer. The main advantage of this perpendicular spin polarizer is to induce a large spin transfer force even at zero magnetic field, thus leading to a record emitted power (up to 0.6 μW) associated to a very narrow spectral linewidth of a few hundreds of kHz. The characteristics of this hybrid vortex based spin transfer nano-oscillator obtained at zero field and room temperature are of great importance for applications based on rf spintronic devices as integrated and tunable microwave source and/or microwave detector. © *2014 AIP Publishing LLC*.
[http://dx.doi.org/10.1063/1.4885537]

The spin transfer effect allows to generate magnetization precessions at the microwave range in a magnetic layer by injecting a dc current through a spin valve (SV) or a magnetic tunnel junction (MTJ).[1,2] The magnetization dynamics are associated with the variation of the magneto-resistance, leading to an ac voltage that oscillates at the same rf frequency.[3,4] These spin transfer driven dynamic effects are directly used in nano-oscillators, also called Spin Transfer Nano-Oscillators (STNOs), for which the frequency can be swept over a large frequency range (e.g., wireless telecommunication frequency range) by changing the injected dc current amplitude.[5] However, for the targeted applications as future rf devices, the spectral features of STNOs such as the emitted power and the quality factor must be improved.[6] So far, the precessional regime associated with spin torque phenomena usually exists only if a large external field is applied,[7–10] which is detrimental for applications. In order to address simultaneously these three crucial issues, the spin torque excitation associated to a magnetic vortex is promising.[11,12] In fact, STNOs based on a magnetic tunnel junction in which a magnetic vortex is excited in the free magnetic layer demonstrated so far the best rf features as far as linewidth and power of the emitted signal are concerned.[13] On one hand, the largest spin transfer force has been predicted to be obtained with a polarizer uniformly and entirely magnetized perpendicularly to the layer plane.[14] However, in such case, it is anticipated that the change of magnetization in time when the vortex core oscillates, and the associated emitted power, is zero.[15] On the other hand, the largest magnetoresistance oscillation shall be obtained with a reference layer uniformly in-plane magnetized, but this would not produce any sustained spin transfer induced oscillations of the vortex. In this work, we study the emission properties measured in a hybrid SV-MTJ system composed of a free magnetic layer being in a vortex state that is sandwiched between a spin polarizing layer with a perpendicular uniform magnetization and a reference layer with an in-plane uniform magnetization. This complex stacking allows us to record very large power emission without any external magnetic field. These results represent a breakthrough in the implementation of such MTJs in rf spintronic systems for telecommunication and detection applications, and even for the design of interacting oscillator network in neuro-inspired processor architectures.[16]

The studied structures are hybrid SV-MTJ samples grown by sputtering deposition: //Ir-Mn 9/CoFe 2.5/Ru 0.85/CoFeB 3/CoFe 0.5/MgO 1.1/CoFe 0.5/CoFeB 1.3/NiFe 10/Co 0.6/Cu 5/$[Co\ 0.2/Ni\ 0.5]_{10}$/Ta 5/Ru 5 (nm). The nanopillar radius of R = 330 nm has been chosen in order to get a magnetic vortex as the remanent magnetic state in the free layer (FL) (that is composed of CoFe/CoFeB/NiFe) (see Fig. 1). The [Co/Ni] stack has its magnetization oriented perpendicular to the plane and is labeled perpendicular spin polarizer (PSP) as it polarizes the electron spins flowing through the Cu spacer to the NiFe vortex layer. The bottom Ir-Mn/CoFe/Ru/CoFeB/CoFe stack is a standard synthetic antiferromagnet (SAF) and plays the role of the reference layer for the MTJ thanks to the uniform in-plane magnetization of SAF CoFeB/CoFe top layers. Despite the complex stacking of these hybrid SV-MTJs, we succeed in preserving a large tunnel magnetoresistance (TMR) of about 65% (at 10 mV) at room temperature. In order to excite a sustained gyrotropic motion of the vortex core, we inject a dc current

[a)]Present address: Department of Physics, ETH Zurich, Zurich, Switzerland.
[b)]Author to whom correspondence should be addressed. Electronic mail: eva.grimaldi@thalesgroup.com
[c)]Present address: Instituto de Fisica - UFRJ, Rio de Janeiro (RJ), Brazil.
[d)]Present address: Service de Physique de l'Etat Condensé (CNRS URA 2464), CEA Saclay, 91191 Gif-sur-Yvette, France.
[e)]Present address: Samsung Electronics, Semiconductor R&D, San Jose, California, USA.

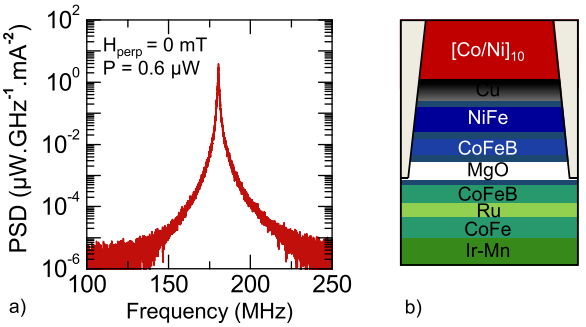

FIG. 1. (a) PSD of the hybrid MTJ vortex based oscillator emission signal at zero magnetic field for $I_{dc} = 15$ mA. (b) Composition of the stacking of the hybrid spin transfer vortex based oscillator. The PSP (red layers) within the spin valve stack is responsible for the excitation of the vortex gyrotropic mode at zero field in the FL (blue layers). The SAF (green layers) top layer magnetization is fixed and allows the detection of the vortex magnetization dynamics within the MTJ.

I_{dc} through the structure that in our convention is positive when electrons are flowing from the SAF to the PSP. All the measurements were performed at room temperature.

The most important result of this study is presented in Fig. 1 and corresponds to the measurement of the rf signal associated to the spin transfer induced gyrotropic motion of the vortex core obtained at zero field. Before performing the rf measurements, the system is initialized by applying $I_{dc} = 15$ mA and a large perpendicular field $\mu_0 H_{perp} = -600$ mT with the aim to set the vortex core direction and the PSP magnetization direction by the direction of the magnetic field, and also set the vortex chirality through the dc current induced Oersted field. The magnetic field is then swept down to zero. The power spectral density (PSD) is recorded with a spectrum analyzer. The peak PSD is fitted with a Lorentzian curve and results in an integrated power of 0.6 μW, a linewidth Δf of 590 kHz, and a frequency f of 180 MHz. We emphasize that the largest emitted power is obtained at zero field in these hybrid SV-MTJ devices.

We now focus on the evolution of these microwave properties, i.e., frequency f, power, and linewidth Δf as a function of the applied external field $\mu_0 H_{perp}$. As shown in Fig. 2(a), for $\mu_0 H_{perp}$ between -21 and 12 mT, the rf spectrum is composed of a single peak (similar to the measurement at zero field) and the frequency varies almost linearly with H_{perp} due to the field-dependent vortex stiffness.[17] In this low field range, the emitted power remains almost constant, close to its maximum value reached around $\mu_0 H_{perp} = 0$ mT (Ref. 18) and the linewidth remains close to

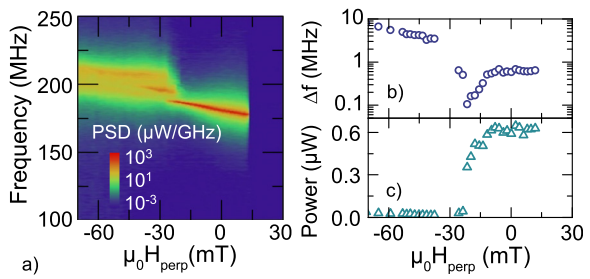

FIG. 2. (a) Power spectrum measured for $I_{dc} = 15$ mA as a function of the external magnetic field $\mu_0 H_{perp}$. Evolution of (b) the spectral linewidth, and of (c) the integrated power as a function of $\mu_0 H_{perp}$ for $I_{dc} = 15$ mA.

its minimum value between 105 kHz and 685 kHz as shown in Figs. 2(b) and 2(c). The linewidth minimum is not obtained at zero field but at $\mu_0 H_{perp} = -21$ mT, corresponding to an effective Q factor of about 1800 defined as $\Delta f/f$ (with $\Delta f = 105$ kHz for $f = 182$ MHz). For larger negative perpendicular fields ($\mu_0 H_{perp} \leq -21$ mT), multiple peaks are observed associated with low emitted power of the order of 10 nW, and large linewidth between 1 and 10 MHz (see Fig. 2(a)).

In order to clearly understand these different emission regimes, we investigate the associated magnetization state in each magnetic layer with measurements of resistance versus field at low current $I_{dc} = 0.1$ mA, so that the magnetic states are not perturbed neither by the Oersted field nor by the spin transfer forces. At large negative fields (see blue curve in Fig. 3), both the magnetization of the FL and of the SAF top layer are pointing downward out-of-plane corresponding to a low resistance magnetic configuration because of the low resistance parallel-like magnetization configuration. When sweeping $\mu_0 H_{perp}$ from -700 mT to 0 mT, the resistance increases as the in-plane components of the vortex and the SAF magnetization increase, leading to a less parallel-like configuration. When sweeping the field from 0 mT to 700 mT, we detect two sharp changes of resistance that are related to the reversal of the PSP magnetization (70 mT) and of the vortex core polarity (400 mT) and consequently different magnetic states can be obtained (see the sketches in Fig. 3). These resistance changes are possibly due to a shift of the vortex core position at the reversal of the PSP and/or the vortex core polarity dipolarly interacting: these displacements lead to a detectable variation of resistance thanks to the large TMR ratio. By sweeping the field from large positive field to large negative field, the symmetrical resistance behavior is observed corresponding to a symmetrical behavior of the magnetization state (see orange curve in Fig. 3). At low fields, the nonlinear change of the resistance can be attributed to the in-plane stray field associated with the SAF that interacts with

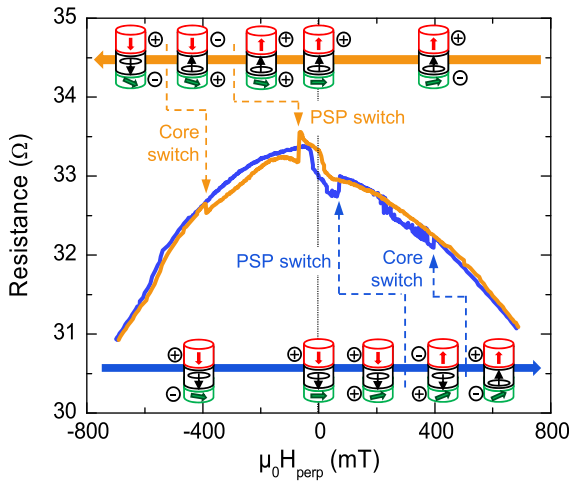

FIG. 3. Resistance versus field measurements for $I_{dc} = 0.1$ mA by (blue) sweeping the field from -700 mT to 700 mT and (orange) from 700 mT to -700 mT. The sketches represent the magnetization of the SAF (green), FL (black), and PSP (red) for increasing (blue arrow) or decreasing (orange arrow) field. The $\oplus$ sign corresponds to a PSP, respectively SAF configuration that favors the STT induced oscillations whereas the $\ominus$ sign corresponds to a configuration where the STT over damps the vortex.

the vortex and is beyond the scope of this Letter. To analyze the variation of the emitted power with the perpendicular field, it is crucial to define precisely the forces acting on the vortex core. In order to understand the balance of forces in the case of the hybrid SV-MTJ system, we first consider the simple case of a Ferromagnetic (F1)/NonMagnetic (NM)/Ferromagnetic (F2) stack that contains only one spin polarizing layer F2 and where the F1 layer has a vortex magnetization distribution. In the case where F2 is a fixed and uniform spin polarizer, the vortex can present spin transfer induced oscillations described by the Thiele equation.[19] Its projection into polar unit vectors gives the critical condition for H_{perp} and current density J^{F2} to obtain sustained oscillations, which corresponds to a counterbalance of the damping by the total spin-transfer force[14]

$$J^{F2} p f_0^{F2}(H_{perp}) p_z^{F2}(H_{perp}) > \frac{D(H_{perp})}{G(H_{perp})} \kappa\left(H_{perp}, J^{F2}\right), \quad (1)$$

with p is the vortex core polarity ($p = \pm 1$), J^{F2} is the current density (positive for electrons flowing from F1 to the spin polarizing layer F2), G is the gyrovector norm ($G > 0$), D is the linear part of the damping coefficient, $f_0^{F2} p_z^{F2}$ is the spin transfer torque efficiency coming from the spin polarizer F2 where $f_0^{F2} = \pi\hbar P_{spin}^{F2}/2|e|$ is the spin transfer torque coefficient (with e is the electric charge, $\hbar$ is the reduced Planck constant, and P_{spin}^{F2} is the spin polarization of the F2 layer) and p_z^{F2} is the out-of-plane component of F2 magnetization, and κ is the linear part of confinement stiffness. These terms are functions of the external perpendicular field and current (for more details, see Appendix in Ref. 20). In a recent work,[13] we established that sustained vortex oscillations are possible only if the spin transfer torque is opposed to the damping that corresponds to $J^{F2} p p_z^{F2} > 0$. In this case, the spin polarized current acts as anti-damping term. Else the spin polarized current has an extra-damping effect that overdamps of the system.

In the case of the hybrid SV-MTJ stack, the PSP layer is designed in order to be the spin polarizing layer at zero field. However, when a perpendicular field is applied, the SAF magnetization is tilted out-of-plane and also acts as an effective spin polarizing layer in the excitation or damping of the vortex free layer magnetization.[13] Consequently, these two distinct layers generate spin polarized current. In this study, as the thickness of the free layer is larger than its spin diffusion length, the spin polarization from the PSP and the SAF are assumed to be independent. Thus, the hybrid SV-MTJ stack is considered in the following as a superposition of two STNOs. The current density used for the measurements, $J_{dc} = I_{dc}/\pi R^2$, is defined positive for electrons flowing from the SAF to the PSP. Compared to the previous discussion with a single F1/NM/F2 stack, the conditions of oscillations become different for the spin valve and for the MTJ. Indeed, from the spin valve point of view, $J^{PSP} = J_{dc}$ and from the MTJ point of view, $J^{SAF} = -J_{dc}$. Thus, the spin transfer torque from the PSP is opposed to the damping if $J_{dc} p p_z^{PSP} > 0$ whereas the spin transfer torque from the SAF is opposed to the damping if $J_{dc} p p_z^{SAF} < 0$. In particular, the out-of-plane component of the SAF top layer magnetization is along the external field direction as $p_z^{SAF} = H_{perp}/4\pi M_s^{SAF}$ (with M_s^{SAF} is the saturation magnetization of the SAF), and the PSP is fully saturated out-of-plane with $p_z^{PSP} = \pm 1$. Knowing the switching field of the PSP magnetization p_z^{PSP}, of the vortex core polarity p and the orientation of the SAF magnetization p_z^{SAF}, we obtain different conditions where the PSP and/or SAF induced spin polarized current act as an anti-damping or an extra-damping torque for the vortex gyrotropic motion. The action of each spin polarizing layer on the vortex sustained dynamics is schematized in the sketches in Fig. 3: $\oplus$ when the STT sustained dynamics is favored and $\ominus$ when the system is overdamped. Considering the rf measurements presented before in Fig. 2 (corresponding to the blue case in Fig. 3), one can see that for large negative fields the spin polarized current due to the SAF top layer acts as an extra-damping term, opposed to the anti-damping effect due to the spin transfer force generated by the PSP layer. Thus, from -500 mT up to -21 mT, we are not able to detect a large rf peak associated large amplitude oscillations, but instead observe multiple FMR modes, due to the extra-damping effect from the SAF layers. By sweeping the field to 0 mT, the out-of-plane component of the SAF magnetization decreases and so does the SAF extra-damping spin polarized current, whereas the anti-damping spin polarized current coming from the PSP layer remains the same: above a critical field ($\mu_0 H_c = -21$ mT), large amplitude vortex core oscillations are induced. For $\mu_0 H_{perp} > 0$ mT, as long as the PSP is not switched, both the PSP and the SAF torques act as anti-damping terms, resulting in an increase of the radius of vortex oscillations and thus to a larger emitted power (see Fig. 2(c)). At $\mu_0 H_{perp} = 15$ mT, because the magnetization of the PSP layer switches, the spin transfer torque coming from the PSP changes its sign and becomes an extra-damping term whereas the anti-damping spin transfer torque coming from the SAF is, in this small field range, too small to counterbalance the effect of the PSP. As a consequence, the vortex oscillations are over damped and the emitted signal is turned-off. Note that in this configuration, large amplitude oscillations are expected for a negative current. However, we were not able to reach this regime in the measurements because of the non-symmetric behavior of the MTJ for which a negative current with the same amplitude leads to damage the junction quality.

Considering the different forces acting on the vortex core in the hybrid SV-MTJ device, the condition to obtain sustained oscillations given by Eq. (1) in the case of a single spin polarizing layer, becomes

$$J_{dc} p \left(f_0^{PSP} p_z^{PSP} - f_0^{SAF} \frac{H_{perp}}{4\pi M_s^{SAF}} \right) > \frac{D}{G} \kappa, \quad (2)$$

with these terms depending on H_{perp} and J_{dc} as already mentioned above. Thus, we solve Eq. (2) to find the region for which the oscillations are sustained. In Fig. 4, we plot in color the critical conditions ($\mu_0 H_{perp}$, I_{dc}) for sustained oscillations for the case where PSP and the vortex core are pointing downward ($p_z^{PSP} = p = -1$), for a SAF spin polarization of $P_{spin}^{SAF} = 0.26$ and for different values of the PSP spin polarization P_{spin}^{PSP}.

Comparing to the experiments presented in Fig. 2 where $I_{dc} = 15$ mA (see dotted line in Fig. 4), we can estimate the

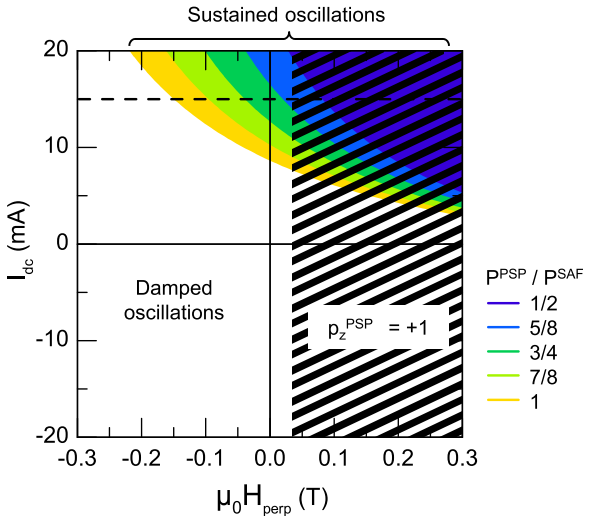

FIG. 4. Conditions of current I_{dc} and field H_{perp} for sustained oscillations (colored region) for the vortex core and the PSP pointing downwards for $P_{spin}^{SAF} = 0.26$ and different values of P_{spin}^{PSP}. The dotted line corresponds to 15 mA. The striped area is a nonrealistic region because of the nonstable downward PSP magnetization.

ratio of the SAF and PSP spin polarization from the critical field $\mu_0 Hc$. If the critical field for oscillations corresponds to the measured field $\mu_0 H_c = -21$ mT at which large amplitude oscillations appear, it corresponds to a spin polarization of the PSP being $3/4\, P_{spin}^{SAF} < P_{spin}^{PSP} < 5/8\, P_{spin}^{SAF}$.

In conclusion, we demonstrate that spin transfer induced vortex oscillations with a perpendicular spin polarizer lead to large amplitude oscillations at relatively low critical current and in absence of external magnetic field. The geometry we have designed allows the excitation of vortex core oscillations, and yields its best microwave features, without any external magnetic field. A maximum emitted power of 0.6 μW and a linewidth of 590 kHz have been obtained at zero field and room temperature. Despite the complexity of our vortex based hybrid SV-MTJ systems, we succeed to provide a complete description of the evolution of the different contributions of the spin transfer forces as a function of field, that helps to optimized the rf emitted signal. Finally, we believe that the rf characteristics of these vortex based hybrid SV-MTJs represents a real breakthrough towards the actual implementation of such spintronics devices in future telecommunications systems.

The authors acknowledge Y. Nagamine, H. Maehara, and K. Tsunekawa of CANON ANELVA for preparing the MTJ films, the financial support from ANR agency (SPINNOVA ANR-11-NANO-0016) and EU FP7 grant (MOSAIC No. ICT-FP7- n.317950). Financial support from CNES and DGA is acknowledged by E.G. and from JSPS by B.R.S.

[1]B. Hillebrands and A. Thiaville, *Spin Dynamics in Confined Magnetic Structures III*, Topics in Applied Physics Vol. 101 (Springer, Berlin, New York, 2006).
[2]D. C. Ralph and M. D. Stiles, J. Magn. Magn. Mater. **320**, 1190 (2008).
[3]S. I. Kiselev, J. C. Sankey, I. N. Krivorotov, N. C. Emley, R. J. Schoelkopf, R. A. Buhrman, and D. C. Ralph, Nature **425**, 380 (2003).
[4]W. Rippard, M. Pufall, S. Kaka, S. Russek, and T. Silva, Phys. Rev. Lett. **92**, 027201 (2004).
[5]A. Slavin and V. Tiberkevich, IEEE Trans. Magn. **45**, 1875 (2009).
[6]B. Georges, J. Grollier, V. Cros, A. Fert, A. Fukushima, H. Kubota, K. Yakushijin, S. Yuasa, and K. Ando, Phys. Rev. B **80**, 060404 (2009).
[7]S. Sani, J. Persson, S. M. Mohseni, Y. Pogoryelov, P. K. Muduli, A. Eklund, G. Malm, M. Käll, A. Dmitriev, and J. Åkerman, Nat. Commun. **4**, 2731 (2013).
[8]H. Maehara, H. Kubota, Y. Suzuki, T. Seki, K. Nishimura, Y. Nagamine, K. Tsunekawa, A. Fukushima, H. Arai, T. Taniguchi, H. Imamura, K. Ando, and S. Yuasa, Appl. Phys. Express **7**, 023003 (2014).
[9]H. Maehara, H. Kubota, Y. Suzuki, T. Seki, K. Nishimura, Y. Nagamine, K. Tsunekawa, A. Fukushima, A. M. Deac, K. Ando, and S. Yuasa, Appl. Phys. Express **6**, 113005 (2013).
[10]H. Kubota, K. Yakushiji, A. Fukushima, S. Tamaru, M. Konoto, T. Nozaki, S. Ishibashi, T. Saruya, S. Yuasa, T. Taniguchi, H. Arai, and H. Imamura, Appl. Phys. Express **6**, 103003 (2013).
[11]V. S. Pribiag, I. N. Krivorotov, G. D. Fuchs, P. M. Braganca, O. Ozatay, J. C. Sankey, D. C. Ralph, and R. A. Buhrman, Nat. Phys. **3**, 498 (2007).
[12]K. Yu. Guslienko, J. Nanosci. Nanotechnol. **8**, 3781 (2008).
[13]A. Dussaux, B. Georges, J. Grollier, V. Cros, A. Khvalkovskiy, A. Fukushima, M. Konoto, H. Kubota, K. Yakushiji, S. Yuasa, K. Zvezdin, K. Ando, and A. Fert, Nat. Commun. **1**, 1 (2010).
[14]A. V. Khvalkovskiy, J. Grollier, A. Dussaux, K. A. Zvezdin, and V. Cros, Phys. Rev. B **80**, 140401 (2009).
[15]P. N. Skirdkov, A. D. Belanovsky, K. A. Zvezdin, A. K. Zvezdin, N. Locatelli, J. Grollier, and V. Cros, SPIN **02**, 1250005 (2012).
[16]N. Locatelli, V. Cros, and J. Grollier, Nature Mater. **13**, 11 (2014).
[17]G. de Loubens, A. Riegler, B. Pigeau, F. Lochner, F. Boust, K. Guslienko, H. Hurdequint, L. Molenkamp, G. Schmidt, A. Slavin, V. Tiberkevich, N. Vukadinovic, and O. Klein, Phys. Rev. Lett. **102**, 177602 (2009).
[18]A. Dussaux, A. Khvalkovskiy, P. Bortolotti, J. Grollier, V. Cros, and A. Fert, Phys. Rev. B **86**, 014402 (2012).
[19]B. Ivanov and C. Zaspel, Phys. Rev. Lett. **99**, 247208 (2007).
[20]E. Grimaldi, A. Dussaux, P. Bortolotti, J. Grollier, G. Pillet, A. Fukushima, H. Kubota, K. Yakushiji, S. Yuasa, and V. Cros, Phys. Rev. B **89**, 104404 (2014).